

### 3D MORPHOLOGICAL ANALYSIS OF THE CONNECTIVITY OF A POROUS MEDIUM

Luc DECKER<sup>1</sup>, Dominique JEULIN<sup>1</sup>, Isabelle TOVENA<sup>2</sup>

<sup>1</sup>Centre de Morphologie Mathématique, Ecole des Mines de Paris, 35 rue St-Honoré F77300 Fontainebleau, France

<sup>2</sup>Commissariat à l'Energie Atomique, Centre de Cadarache, Bât 352 F13108 Saint-Paul-lez-Durance Cédex, France

#### ABSTRACT

The connectivity of a complex porous medium is analysed by means of a set of serial sections. From these data, geodesic propagations in different directions provide an estimation of the distribution function of the local tortuosity of shortest paths in the medium, while simulations of random walks give estimates of the effective coefficients of diffusion at different scales and of their anisotropy.

Key words: connectivity, geodesic propagation, tortuosity, diffusion, simulations, porous media, anisotropy.

#### INTRODUCTION

The connectivity of a porous network controls its overall transport properties. Usually global connectivity measurements are available from serial sections analysis, or from a stereological estimation by means of appropriate random sets models. The aim of this study, is to give a direct estimation of the tridimensional tortuosity and diffusion coefficients of a porous medium from a 3D image of a block of material.

#### IMAGES OF THE POROUS MEDIUM

A 110mm cylinder specimen of a porous medium was sectionned into 53 vertical slices parallel to the axis of the cylinder ( $y$  vertical direction), with a 2mm spacing ( $z$  direction). The horizontal direction is named  $x$ . Photographs were made on the sections for further analysis, and scanned into 8 bits digital images with  $(x, y)$  sizes ranging from 1000 x 900 to 2300 x 900 pixels. The distance between two pixels is 2 mm in the section direction  $z$  and 0.051 mm in the two other directions. The morphology of the solid and porous phases is very tortuous.

The reconstruction of the tridimensional specimen required some preliminary image processing. Irregularities in the grey level images, due to the marks of the saw used for cutting the specimen, were filtered by estimation of a local drift on every vertical line. Photographs of successive sections were matched by means of a translation maximizing their correlation (the optimal correlation coefficient ranging from 0.10 to 0.45). The final data basis is a

paralleliped cut into the cylinder, made of 35 matched slices containing each 1436 x 636 voxels. The digital images are then converted into binary images where the pores and the solid phase are separate. This is obtained in two steps: a first threshold enables us to extract the extended porosities, while a morphological top-hat transformation (Serra 1982), followed by a threshold and a reconstruction filter provides the lamellar voids with a higher reflectance.

### 3D GEODESIC PROPAGATIONS IN THE POROUS MEDIUM

In a first step, we are looking for the measurements of morphological properties describing the connectivity and the tortuosity of the porous medium. This type of approach was made in earlier studies, in two dimensions for the diffusion in polymer composites (Jeulin et al., 1992; Gateau et al., 1994) and in three dimensions for the contact between rough surfaces (Demarty et al., 1996) or for sintered materials (Demarty et al., 1997).

Propagation phenomena (light in optics, sound in acoustics, fluid in a porous medium,...) with different propagation velocities in heterogeneous media, involve the existence of paths (namely of percolation) across a specimen. For a valued graph, one can estimate (from images in 2D or in 3D) the distance to a source on the valued graph, usually called the geodesic distance (namely the length of shortest paths), and its probability distribution function, characterizing the tortuosity of a network. In the present case, the connectivity of the porous medium is studied by geodesic propagations from a source and a destination made of two parallel faces. They enable us to calculate the distance of any point in the volume to the source on a cubic graph and on a cubo-octaedric graph (Decker and Jeulin, 1997) with valued edges (1 in pores and  $+\infty$  in grains). Points that cannot be accessed during the propagation are located at the distance  $+\infty$  from the source. From this procedure can be detected closed pores in a specimen. In our situation, the open pore volume fraction is equal to 0.200 while the total pore volume fraction is equal to 0.226; the closed pores are limited to 12% of the total porosity. If the pores percolate through the specimen, the geodesic distance between the two faces is finite. Its value, divided by of their euclidean distance, is a measure of the global tortuosity of the porous medium, while the distribution of geodesic distances inside the specimen or on the arrival plane give details on the tortuosity of the whole shortest paths. This information is collected in a few minutes on a Sparc SUN Workstation, using the XLIM software developed at CMM (Gratin, 1992). To illustrate our results, we show in Fig. 1 the geodesic paths of the specimen with the higher tortuosity (ranging from 1.8 to 2.2), which are localized close to the center of the sample. In Fig. 2 are given the distribution functions of the tortuosities obtained for the cubo-octaedron graph in the  $x$  and  $y$  directions. As expected, the propagation is more direct in the  $x$  direction (where the lower tortuosity is close to 1 and the larger is close to 1.4). In the  $y$  direction, the dispersion of the tortuosities is much larger (they extend from 1.8 to more than 3.4).

### DIFFUSION IN THE POROUS MEDIUM

**Random walks:** The diffusion of a fluid in the pores of the medium can be studied by means of random walks generated from separate particles (Decker and Jeulin, 1997, Tovina et al., 1998). During their walk, the particles follow a Brownian motion with reflecting conditions on the pore walls. In our case, up to  $N = 100000$  particles start at time  $t_0 = 0$  from open pores located in an ellipsoid with axis  $r_x = 300$ ,  $r_y = 100$  and  $r_z = 3$ ,

with uniform coordinates  $(x_0, y_0, z_0)$ . At every time step, the current particle moves on the cubic grid from the location  $(x(t), y(t), z(t))$  to the location  $(x', y', z')$  where every new coordinates is obtained by a random choice according to the following probabilities (if the new location is outside the pores, the particle keeps its location):

$$\begin{cases} P[x' = x(t) + 1] = p_x & P[x' = x(t)] = p_{o_x} & P[x' = x(t) - 1] = 1 - p_x - p_{o_x} \\ P[y' = y(t) + 1] = p_y & P[y' = y(t)] = p_{o_y} & P[y' = y(t) - 1] = 1 - p_y - p_{o_y} \\ P[z' = z(t) + 1] = p_z & P[z' = z(t)] = p_{o_z} & P[z' = z(t) - 1] = 1 - p_z - p_{o_z} \end{cases}$$

The probabilities  $p_x, p_y$  and  $p_z$  are fixed and produce a bias in the trajectories of particles as a result of a drift, similar to a main flow. For a homogeneous medium (free diffusion of particles in pores), the reference coefficients of diffusion are given from

$$D_x = p_x \quad D_y = p_y \quad D_z = p_z$$

**Estimation of the diffusion coefficient from the variogram of trajectories:** As in (Matheron, 1979; Jeulin, 1992), when a macroscopic Fick's law is observed, the coordinates  $X_i(t)$  ( $i = 1, 2, 3$ ) of the trajectory of the marked particle (starting from  $x_0$  ( $x_{0i}$ ) at time  $t = 0$ ) in the random velocity field  $u(x)$  are diffusion stochastic processes with expectation and covariance given by

$$E[X_i(t)] = x_{0i} + \bar{u}_i t \tag{1}$$

$$E[(X_i(t) - x_{0i} - \bar{u}_i t)(X_j(t) - x_{0j} - \bar{u}_j t)] = 2D_{ij}t \tag{2}$$

where  $\bar{u}_i$  is the average of the  $i$  component of the velocity, while the coefficients  $D_{ij}$  build the effective diffusion tensor of an equivalent homogeneous porous medium. Equivalently for a single coordinate (e.g.  $x$ ) we have the variogram  $2\gamma_x(t)$ :

$$2\gamma_x(\Delta t) = E[(X(t + \Delta t) - X(t))^2] = 2D_x\Delta t + u_x^2(\Delta t)^2$$

The macroscopic coefficients  $\bar{u}_i$  and  $D_{ij}$  obtained from averages of many particles trajectories are valid for an equivalent homogeneous medium when are fulfilled the conditions for a macroscopic Fick's law to exist; these conditions are unknown in general. For some random media (for instance for self similar, and therefore non stationary porous networks), Eqs (1,2) are not valid, and a  $At^\alpha$  (with  $\alpha \neq 1$ ) behaviour is observed (this is called anomalous diffusion). This can also be reinterpreted as a change of the coefficient of diffusion with time (with an effective coefficient  $D \sim At^{\alpha-1}$ ), and consequently with the scale of observations.

**Estimation of the diffusion coefficient from the distribution of sojourn times:**

Additional information is obtained from the empirical distribution of the sojourn time  $\tau$  of the particle in the simulated field,  $F_{\tau_a}(t)$ . If we consider particles starting from  $O$  and leaving the field at the abscissa  $a$  at time  $\tau_a$ , we expect in the case of a constant velocity field  $(u_x, u_y)$  and in an infinite homogeneous medium:

$$F_{\tau_a}(t) = P\{\tau_a < t\} \tag{3}$$

We have:  $X(t) \geq a \Rightarrow \tau_a \leq t$  and therefore

$$P\{X(t) \geq a \mid \tau_a < t\} = \frac{P\{X(t) \geq a\}}{F_{\tau_a}(t)} \tag{4}$$

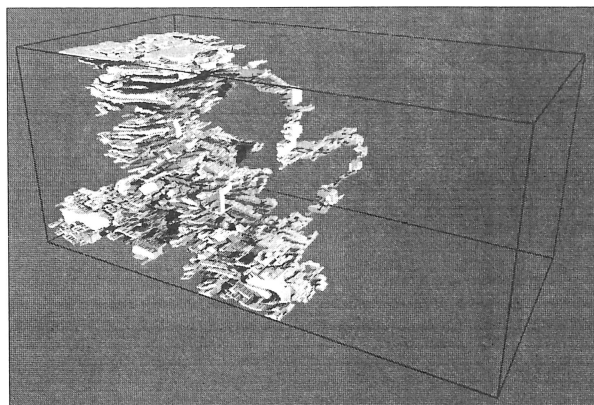
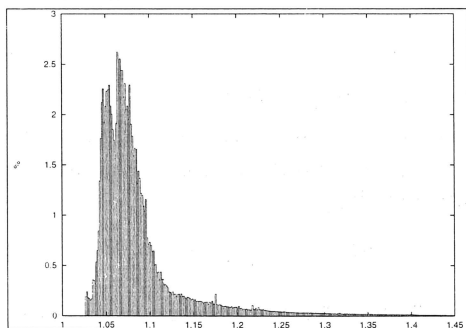
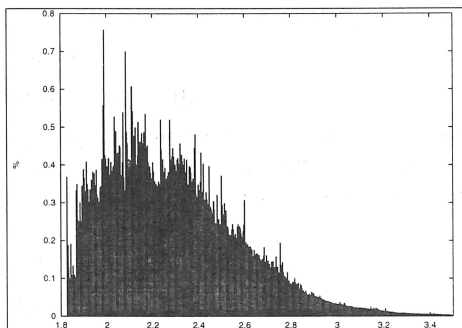


Figure 1: Set of the shortest paths (tortuosity from 1.8 to 2.2) for the percolation in the vertical direction  $y$

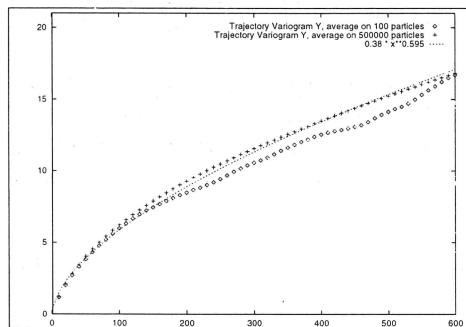


Crossing in horizontal direction  $x$

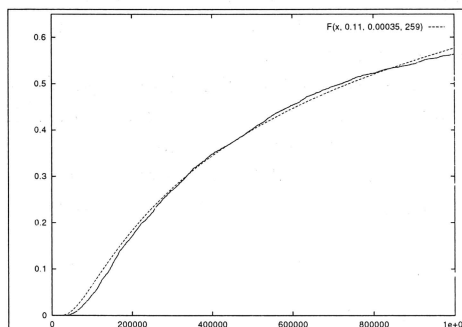


Crossing in vertical direction  $y$

Figure 2: Histograms of the tortuosity obtained by geodesic propagations



Fit of the trajectory variogram



Fit of the sojourn time distribution

Figure 3: Results of the random walk simulations for the estimation of  $D_y$

If  $u_x = 0$ , by symmetry we have  $P\{X(t) \geq a \mid \tau_a < t\} = \frac{1}{2}$  and in these conditions

$$F_{\tau_a}(t) = 2P\{X(t) \geq a\} \tag{5}$$

When  $u_x \gg 0$  and  $a > 0$ ,  $P\{X(t) \geq a \mid \tau_a < t\} \simeq 1$  and

$$F_{\tau_a}(t) = P\{X(t) \geq a\} \tag{6}$$

In Eqs. (5,6) the probability  $P\{X(t) \geq a\}$  for a Brownian motion with the drift  $u_x$  is obtained by

$$P\{X(t) \geq a\} = \frac{1}{\sqrt{4\pi D_x t}} \int_a^{+\infty} \exp - \left( \frac{(x - u_x t)^2}{4D_x t} \right) dx \tag{7}$$

This method is interesting to estimate long time (and therefore large scale) coefficients of diffusion, the particles being allowed to sample a large part of the specimen before they leave the specimen. When closing the boundaries of the domain in one or two directions, we can measure sojourn times  $\tau_a$  in the other directions (Decker and Jeulin, 1997).

This method was applied to the porous specimen, with the probabilities  $p_{0_x}$ ,  $p_{0_y}$  and  $p_{0_z}$  set to 0.20. Biased and unbiased (resulting into  $\bar{u} = 0$ ) walks were used. For the sojourn time distribution, a bias in the wanted direction is used (for instance  $p_x = 0.4 - 0.5$ ). An experimental variogram, and the cumulative distribution of sojourn times corresponding to Eq. 7 are given for the  $y$  direction are given in Fig. 3. It turns out that the Fick's law is an approximation, the coefficient  $\alpha$  differing from 1 in certain directions (in  $x$  and mainly in  $y$ ): we obtained after fitting the data  $\gamma_x(t) \simeq 0.19t^{0.95}$  and  $\gamma_y(t) \simeq 0.38t^{0.60}$ . Therefore at a small scale (2 - 4mm) the diffusion behaviour is 'underdiffusive' with respect to the Fick's law, as a result of particles being trapped, and slowed in elongated pores. In addition, the coefficients estimated by the two methods (variograms and sojourn times) differ, since they are related to different scales, as illustrated in Tbl.1 (where the errors correspond to the fit of the experimental curves). The coefficients of diffusion increase with the scale of observation, the long range connectivity of the porous medium appearing on the larger scale. The coefficient of diffusion  $D_y$  is much lower than for the other directions, mainly at the small scale. At the larger scale, it is nearly twice lower, presenting the same coefficient of anisotropy as the tortuosity (the higher the tortuosity, the lower the coefficient of diffusion).

Table 1. Estimated coefficients of diffusion

		Fick's law approximation	non linear variogram
$D_x$	small scale: 4 mm	$0.13 \pm 0.01 \text{ pixels}^2 [T^{-1}]$	$0.14 \pm 0.01 \text{ pixels}^2 [T^{-1}]$
	large scale: 70 mm	$0.23 \pm 0.05 \text{ pixels}^2 [T^{-1}]$	
$D_y$	small scale: 2 mm	$0.025 \pm 0.010 \text{ pixels}^2 [T^{-1}]$	$0.028 \pm 0.010 \text{ pixels}^2 [T^{-1}]$
	large scale: 30 mm	$0.11 \pm 0.03 \text{ pixels}^2 [T^{-1}]$	
$D_z$	small scale: 20 mm	$0.09 \pm 0.03 \text{ pixels}^2 [T^{-1}]$	
	large scale: 70 mm	$0.14 \pm 0.02 \text{ pixels}^2 [T^{-1}]$	

CONCLUSION

The direct tridimensional estimation of the connectivity, the tortuosity and of the diffu-

alternative, and more stereological way to simplify the experimental part of the study, would be to first estimate from sections the parameters of a 3D random set model representing the porous medium, and then to make the connectivity measurements on 3D simulations of the medium.

#### REFERENCES

- Decker L, Jeulin D. N.10/97/MM, 1997, Paris School of Mines publication.
- Demarty CH, Grillon F, Jeulin D. Study of the contact permeability between rough surfaces from confocal microscopy. *Microscopy, Microanalysis, Microstructure* 1996; 7: 505-511.
- Demarty CH, Jeulin D, L'Espérance G, Perrier E. 3D morphological analysis of the connectivity of a sintered material. *Cell Vision* 1997; 4.2: 218-219.
- Gateau P, Jarrin J, Brémond R, Jeulin D, Serpe G. Estimation of the transport properties of polymer composites by geodesic propagation. *Journal of Microscopy* 1994; 176:167-177.
- Gratin C. Xlim3d : un logiciel de traitement d'images tridimensionnelles. N.9/92/MM, 1992, Paris School of Mines publication.
- Gratin C, Meyer F. Morphological three-dimensional analysis. *Scanning Microscopy Supplement* 1992: 129-135.
- Jeulin D. Flow and diffusion in random porous media from lattice gas simulations. In: TMM Verheggen (ed), *Numerical methods for the simulation of multiphase and complex flow*, Berlin: Springer-Verlag, 1992: 106-123.
- Jeulin D, Vincent L, Serpe G. Propagation algorithms on graphs for physical application. *Journal of Visual Communication and Image Representation* 1992; 3: 161-181.
- Matheron G. Quelques exemples simples d'émergence d'un demi-groupe de dispersion, N/CMM-599, 1979, Paris School of Mines publication.
- Serra J. *Image Analysis and Mathematical Morphology*. London: Academic Press, 1982.
- Tovena I, Decker L, Jeulin D, Pocachard J, Ragot C. Simulation of water diffusion in packed metallic waste, Communication to the Waste Management Symposium, Tucson, USA (1-5 March 1998).